Magnetic moments of low-lying states in ^{103}Rh, ^{111,113}Cd, and ^{123,125}Te

N. Benczer-Koller, G. Lenner,* R. Tanczyn, A. Pakou,† G. Kumbartzki, A. Piqué, D. Barker,‡ D. Berdichevsky, and L. Zamick
Department of Physics, Rutgers University, New Brunswick, New Jersey 08903
(Received 10 January 1989)

The magnetic moments of several short-lived states in ^{103}Rh, ^{111,113}Cd, and ^{123,125}Te isotopes have been measured by the transient field technique. The results, together with those obtained earlier in the ^{107,109}Ag isotopes, have been compared to predictions of various models and calculations. In the $Z=45,47$ isotopes, the odd proton seems to deform the vibrational core. The data are best explained within the framework of a triaxially deformed nucleus. In the odd-neutron isotopes with $50<N<82$ and $Z=48,52$, weak-coupling states coexist with single-particle states in a mix of configurations.

I. INTRODUCTION

The determination of electromagnetic moments of nuclear states has helped to elucidate the underlying structure of these states because the moments reflect directly the shape and nucleon configuration of the nucleus studied. In particular, magnetic moments distinguish easily between single-particle configurations and collective states and, furthermore, are able to clearly point out whether neutron or proton excitations are responsible for the observed structure. The advent of techniques combining nuclear hyperfine interactions with magnetic properties of solids has allowed the determination of magnetic moments of very short-lived nuclear states.[1] Magnetic hyperfine fields of the order of tens of Teslas can be obtained and therefore spin-aligned states with lifetimes of the order of fractions of picoseconds can be induced to precess by measurable angles of the order of milliradians. The transient field experienced by fast nuclei traversing ferromagnetic media is one of the highest hyperfine fields achievable in the laboratory. The technique has been thoroughly exploited over the last 20 years and has proved particularly successful in the study of even-even nuclei.[2]

Precision measurements of many magnetic moments of short-lived states in nuclei covering the whole periodic table have been obtained, and considerable understanding of nuclear structure details has been achieved. New effects, such as the occurrence of shell closure at $Z=64$ for $N<88$, have been investigated.[3] The extension of such studies to odd nuclei was slow in developing because of a number of technical difficulties which will be described in the next section. Nevertheless, a few cases of medium-weight,[4–6] as well as heavy odd nuclei, have been investigated recently.[7–9]

The moments of the 2_1^+ states of even-even nuclei in the region of $50\leq N\leq 82$ and $44\leq Z\leq 58$ have been very successfully evaluated in terms of the interacting boson approximation (IBA). The clearest treatment of the odd nuclei in this region handles the interaction of the odd nucleon with the excitations of the neighboring even core via the empirical weak-coupling scheme proposed by de Shalit.[10] However, except for the original case of ^{197}Au, the weak-coupling model has, at best, provided only a qualitative description of the nuclear motions and alternate models have been investigated. The interplay of the odd nucleon with the collective excitations of the core has been analyzed by coupling the single particle to a symmetric or an asymmetric rotor,[11] as well as within the context of the interacting boson-fermion model (IBFM).[12–14]

Section II describes briefly the experimental problems that need to be solved in order to carry out these measurements. Section III outlines the results obtained for the odd-proton nucleus ^{103}Rh, and for the odd-neutron nuclei, ^{111,113}Cd and ^{123,125}Te. The results for ^{107,109}Ag have been obtained previously by three different groups[4–6] and are included for comparison. Finally, Sec. IV contains a discussion of these measurements. Preliminary results have already been reported in various conferences.[15–18]

II. EXPERIMENTAL DETAILS

The details of the experimental layout and analysis procedures have been described extensively in many publications.[2,4] Only the traits that differentiate the studies of odd nuclei from those of even nuclei and the particulars of the present experiment will be outlined here.

(i) The low-lying energy levels in odd nuclei are more closely spaced than in even nuclei. Hence, high resolution Ge detectors have to be used.

(ii) The transitions to the levels of interest in odd nuclei tend to be $M1$ rather than $E2$, and therefore the states are weakly populated in Coulomb excitation.

(iii) The angular distributions of the decay gamma rays in coincidence with backscattered particles are very pronounced in the case of the even nuclei. However, for the odd nuclei, these correlations are much weaker. Since the effect to be measured is directly proportional to the slope of the angular correlation at the particular angle where the measurement is taken, the anticipated effects are much smaller than for the corresponding even nuclei. In addition, if the ground state spin is larger than $\frac{3}{2}$, the angular correlation is nearly isotropic and nuclear precession experiments will not yield reliable results.

These effects conspire to reduce the counting rates. In order to obtain similar statistics as those obtained for even nuclei, much longer running times are required, namely 10–20 days instead of several hours. Aside from these differences, the general experimental approach is quite similar to that used for the even nuclei.

The levels of interest were Coulomb excited by 72–80 MeV ^{32}S beams from the Rutgers Tandem Van de Graaff accelerator. The coincidence rate between ^{32}S ions backscattered into an annular surface barrier detector and gamma rays detected in four NaI(Tl) or Ge crystals was recorded.

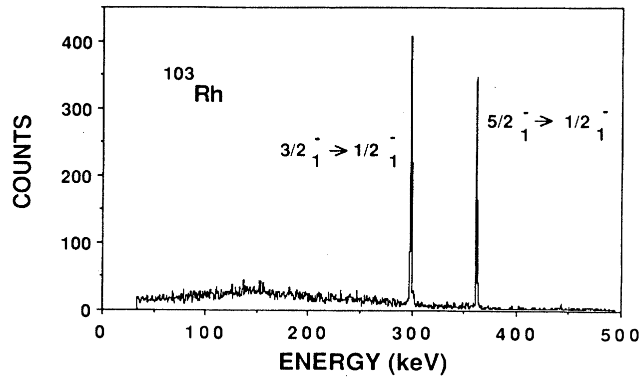

FIG. 1. Coincidence gamma-ray spectrum for ^{103}Rh measured with Ge detectors.

A. Target preparation

Triple layered targets were used for the experiments described in this paper. These were prepared by evaporating the isotope under study on thin iron foils backed by copper thick enough to stop the recoiling nuclei. The iron foils were first rolled to the desired thickness and then annealed at 800 °C for one hour in a hydrogen atmosphere. The magnetization of the foils was measured before and after each run in an ac magnetometer.[19] No beam induced deterioration of the foil magnetization was observed.

Evaporation of the isotope at close range of the electron gun caused the targets to be nonuniform in thickness. Hence, the actual thicknesses of the isotope layer were measured by Rutherford backscattering of 20 MeV ^{12}C beams. The target was translated across the beam in order to determine the thickness profile. The target thicknesses determined by this procedure are listed in Table I which displays, in addition, the target parameters, and the beam and recoil nucleus kinematics relevant to the calculation of g factors. It should be noted, however, that the final result is insensitive to the target thickness. For example, a doubling of the target thickness causes only a 10% change in the g factor.

B. Gamma-ray detectors

Four 17.6 cm by 17.6 cm NaI(Tl) detectors were used for the Cd isotopes, but four Ge detectors ranging in efficiency from 6% to 30% of the efficiency of comparable NaI(Tl) detectors at 1.33 MeV were needed for the other nuclei. Particle-gamma coincidence spectra are displayed in Figs. 1–3. For the precession runs, the gamma-ray detectors 2 and 3 were placed at angles $\vartheta = \pm 57°$ or $\pm 62°$ and detectors 1 and 4 at angles $\vartheta = \pm 123°$ or $\pm 118°$ where the slopes of the relevant particle-gamma angular correlations are appreciable.

TABLE I. Summary of target configurations and kinematics of the recoiling ion. l is the thickness of the target isotope. L is the thickness of the iron layer. M is the magnetization of the ferromagnetic layer in an external field $H_{ext} = 0.0625$ T. v/v_0 is the ion velocity in units of the Bohr velocity $v_0 = e^2/\hbar$.

Target Enrichment (%)	Thickness l (mg/cm^2)	Thickness L (mg/cm^2)	Magnetization M (Tesla)	Beam $E(^{32}S)$ (Mev)	Isotope in Ferromagnet E_{in} (Mev)	E_{out} (MeV)	$\left(\frac{v}{v_0}\right)_{in}$	$\left(\frac{v}{v_0}\right)_{out}$
^{103}Rh-1 (nat)	1.13	1.50	0.1678	76.0	41.3	15.9	4.02	2.50
Rh-2 (nat)	1.86	1.70	0.1729	72.5	31.9	8.90	3.53	1.87
Rh-3 (nat)	1.47	1.61	0.1775	76.1	29.5	8.50	3.40	1.82
Rh-4 (nat)	1.59	1.64	0.1706	73.1	32.6	9.71	3.57	1.95
^{110}Cd-1 (96.63)	1.31	2.18	0.1665	77.9	39.4	7.9	3.80	1.70
Cd-2 (96.63)	0.69	1.62	0.1636	77.9	45.9	17.0	4.10	2.49
^{110}Cd-1 (96.05)	1.52	1.55	0.1707	73.0	34.2	11.6	3.53	2.05
Cd-2 (96.05)	0.42	2.42	0.1666	77.5	48.3	9.5	4.19	1.85
^{113}Cd (91.67)	0.66	1.58	0.1759	78.0	45.6	17.7	4.03	2.51
^{123}Te (76.67)	1.29	1.67	0.1604	78.0	37.9	12.4	3.53	2.02
^{125}Te (93.45)	1.36	1.61	0.1616	78.0	37.0	12.7	3.45	2.03

C. Particle-gamma angular correlations

The angular correlations were measured in all cases by setting the four detectors at four different angles and normalizing the observed rates by the relative detector efficiencies. These were in turn determined from the counting rates obtained in the precession measurement in which the detectors were located at the same angles. The correlations were fitted to the function

$$W(\theta)=\sum_{k_{\text{even}}} Q_k B_k(I_1)P_k(\cos\theta)\frac{R_k(\bar{L}\bar{L}I_1I_2)+2\delta R_k(\bar{L}LI_1I_2)+\delta^2 R_k(LLI_1I_2)}{1+\delta^2}\ , \tag{1}$$

where δ is the mixing ratio relevant to the mixed $M1/E2$ transition, $P_k(\vartheta)$ are Legendre polynomials, R_k are coefficients tabulated in the literature,[20] and the coefficients B_k are given by

$$B_k(I_I)=\sum_{M_I=0}^{M_I=I_I} W(M_I)\rho_k(I_I,M_I)\ . \tag{2}$$

ρ_k are statistical tensor coefficients[20] and $W(M_I)$ are the substate population fractions for the states of interest. The parameters δ and $W(M_I)$ are obtained from fits to the data. Q_k are the geometric factors which take into account the finite size of the gamma-ray detectors. These were numerically calculated for each detector. The Q_k's applicable to the Ge detectors are different from each other because of the very different geometry of the four detectors. The maximum spread in Q_k among the four detectors was 2% and 7% for Q_2 and Q_4, respectively. In order to extract the angular correlation parameters from this type of measurement, the Q_k's were averaged. It was ascertained, however, that the fits are not very sensitive to the value of Q_k. Hence this averaging procedure does not alter in a significant manner the determination of the population fraction, which in turn contributes to the determination of the slope of the angular correlation at the angles of interest. Angular correlations are illustrated in Figs. 4–7.

D. Precession measurements

The net precession of the gamma-ray angular correlation under reversal of the external magnetic field was observed from the ratio

$$\rho_{ij}=\left[\frac{N_i^{\uparrow}/N_i^{\downarrow}}{N_j^{\uparrow}/N_j^{\downarrow}}\right]^{1/2}, \tag{3}$$

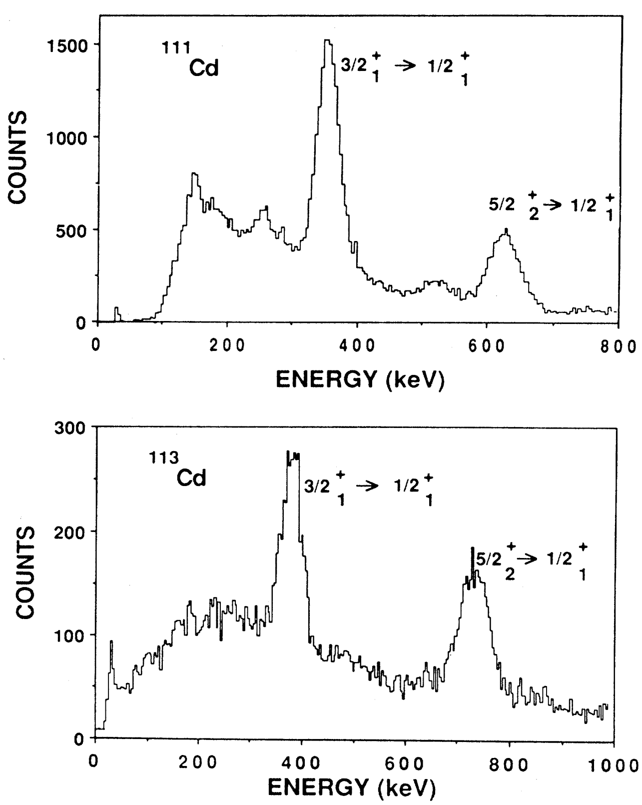

FIG. 2. Coincidence gamma-ray spectra for ^{111,113}Cd measured with NaI(Tl) scintillators.

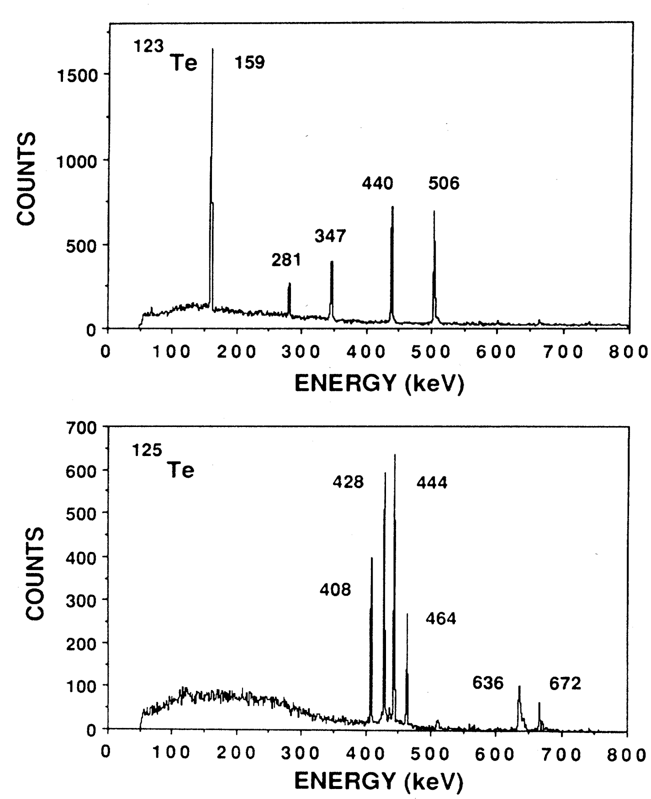

FIG. 3. Coincidence gamma-ray spectra for ^{123,125}Te measured with Ge detectors.

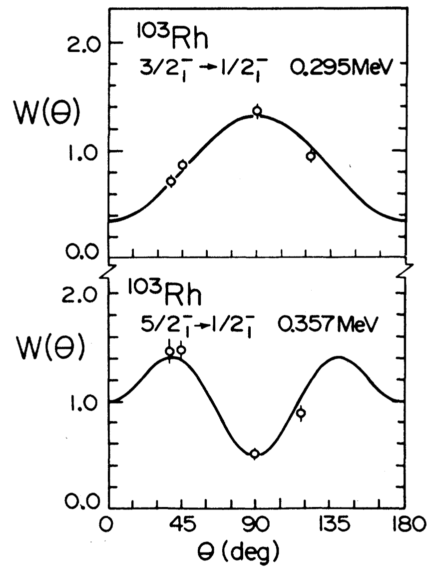

FIG. 4. Measured particle-gamma-ray angular correlations for the $3/2_1^- \rightarrow 1/2_1^-$ and $5/2_1^- \rightarrow 1/2_1^-$ transitions in ^{103}Rh.

where the subscripts $i=1,2$, $j=3,4$ represent the four detectors. $N(\uparrow\downarrow)_{ij}$ is the random- and background-subtracted coincidence counting rate in the photopeak of the ith or jth detector with the external field up or down with respect to the plane of the reaction. The measured effect,

$$\epsilon = \frac{\rho - 1}{\rho + 1} , \tag{4}$$

is related to the desired rotation of the angular distribution $\Delta\vartheta$ by the expression

$$\Delta\vartheta = \epsilon / S , \tag{5}$$

where S is the logarithmic slope of the angular distribution at the angle where the measurement is taken, $S=(1/N)(dN/d\vartheta)$, and $\rho=(\rho_{14}/\rho_{23})^{1/2}$. A summary of the logarithmic slopes S and measured precession angles $\Delta\vartheta$ is presented in Table II.

E. Parametrization of the transient field

The parametrization of the transient field determined by the Rutgers group[2] for the region of ion velocities used in these experiments, $1.6 \leq (v/v_0) \leq 4.5$,

$$B(v,Z) = 96.7(v/v_0)^{0.45} Z^{1.1} M \tag{6}$$

was used to analyze the data of all isotopes except Cd. In that particular case, the g factor of the 2_1^+ state of ^{110}Cd, $g=0.273(17)$ which is known from independent measurements,[21–24] was used as an internal calibration of the transient field. M represents the magnetization of the ferromagnetic foil. Table III shows the experimental g factors and mean lives that were used in obtaining the re-

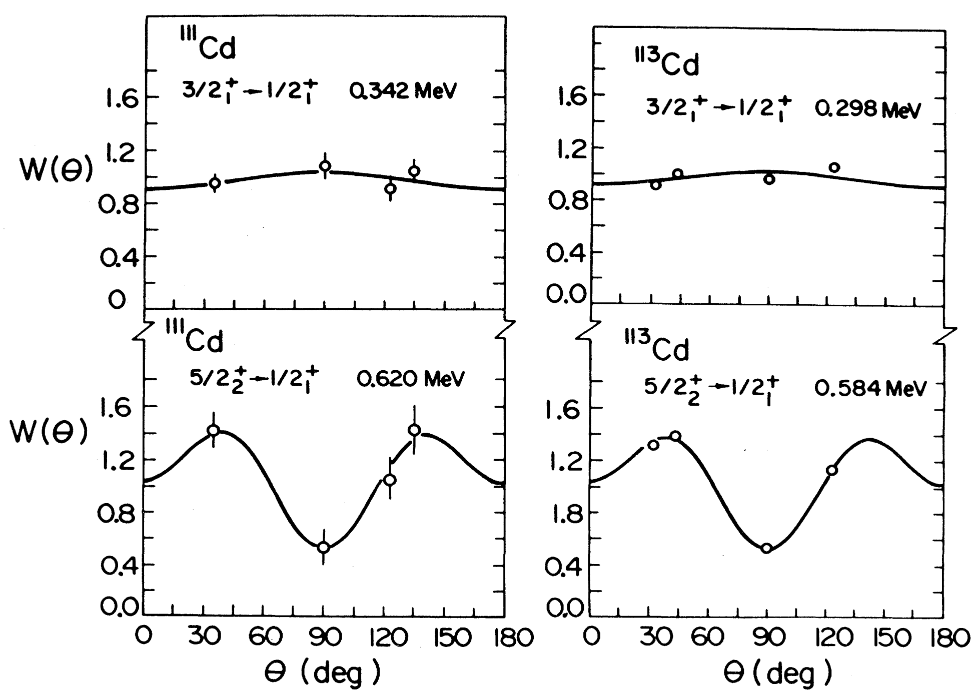

FIG. 5. Measured particle-gamma-ray angular correlations for transitions in ^{111,113}Cd.

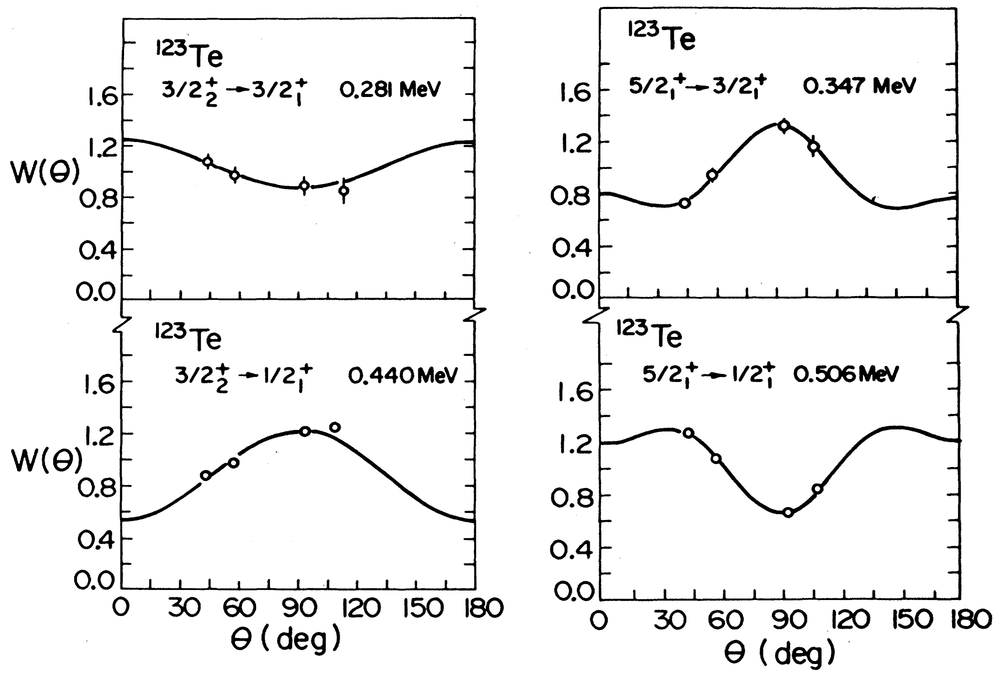

FIG. 6. Measured particle-gamma-ray angular correlations for transitions in ^{123}Te.

sulting $g(2_1^+)$ for ^{110}Cd from which the transient field was calibrated.

The g factor is obtained from the measured angular precession $\Delta\vartheta$, from the expression

$$g = -\Delta\vartheta \Big/ \left[(\mu/\hbar) \int B(t) e^{-t/\tau} dt \right] . \tag{7}$$

The g factors derived from the data and the Rutgers parametrization are given in Table II.

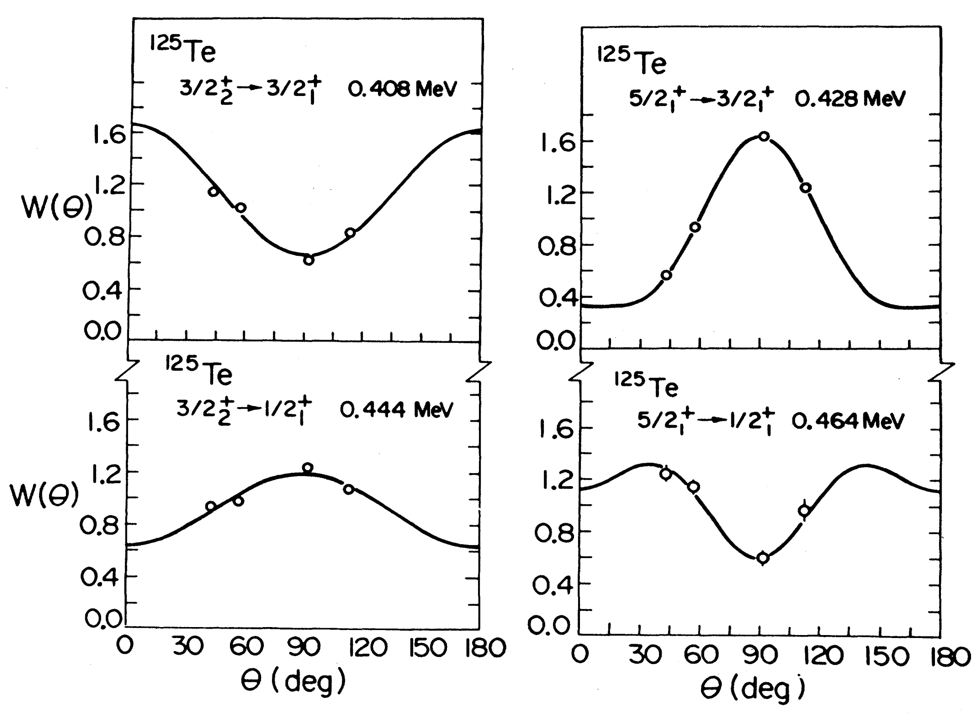

FIG. 7. Measured particle-gamma-ray angular correlations for transitions in ^{125}Te.

TABLE II. Summary of experimental precession angles, logarithmic slopes, and g factors derived from the data and the Rutgers transient field parametrization.

Run	Angle θ (deg)	Slope (θ) $\lvert S\rvert$ (rad^{-1})	Precession $\Delta\theta$ (mrad)	g factor Rutgers parametrization	Slope (θ) $\lvert S\rvert$ (rad^{-1})	Precession $\Delta\theta$ (mrad)	g factor Rutgers parametrization
^{103}Rh:			0.295 MeV, $3/2_1^- \to 1/2_1^-$			0.357 MeV, $5/2_1^- \to 1/2_1^-$	
	51	1.33(9)	−10.1(152)	+0.44(65)	0.733(12)	9.1(220)	−0.40(98)
	57	1.09(7)	−17.1(129)	+0.74(55)	1.074(23)	0.14(1060)	−0.01(47)
	62	0.793(71)	−14.2(96)	+0.48(32)	1.332(71)	−21.1(63)	+0.69(21)
	57	0.975(83)	−18.5(89)	+0.62(30)	1.151(32)	−6.32(680)	+0.21(22)
	57	1.122(59)	−7.8(43)	+0.28(15)	1.121(31)	−6.99(400)	+0.24(14)
	57	1.288(76)	−14.5(30)	+0.52(11)	0.976(24)	−12.7(36)	+0.45(13)
			Average $g(3/2_1^-)=+0.46(8)$			Average $g(5/2_1^-)=+0.37(8)$	
^{111}Cd			0.342 MeV, $3/2_1^+ \to 1/2_1^+$			0.620 MeV, $5/2_2^+ \to 1/2_1^+$	
	57	0.062(27)	−23.3(590)	+0.81(200)	1.088(21)	−10.5(50)	+0.37(17)
	57	0.02(13)	136(891)	−4.7(307)	1.31(12)	−3.2(21)	+0.11(8)
	57	0.132(58)	17.8(888)	−0.44(210)	1.138(37)	−6.0(120)	+0.15(29)
	62	0.120(54)	9.2(740)	−0.24(175)	1.434(63)	−7.5(79)	+0.18(19)
			Average $g(3/2_1^+)=+0.025(1100)$			Average $g(5/2_2^+)=+0.15(6)$	
^{113}Cd:			0.298 MeV, $3/2_1^+ \to 1/2_1^+$			0.584 MeV, $5/2_2^+ \to 1/2_1^+$	
	57	0.105(39)	10.0(410)	−0.36(150)	1.151(18)	−3.3(31)	+0.12(11)
	57	0.161(46)	10.1(235)	−0.36(85)	1.106(21)	−1.4(25)	+0.05(9)
			Average $g(3/2_1^+)=-0.36(74)$			Average $g(5/2_2^+)=+0.08(7)$	
^{123}Te:			0.281 MeV, $3/2_2^+ \to 3/2_1^+$			0.347 MeV, $5/2_1^+ \to 3/2_1^+$	
	57	0.407(81)	−26.3(222)	+0.82(69)	0.913(41)	−1.03(566)	+0.03(18)
			0.440 MeV, $3/2_2^+ \to 1/2_1^+$			0.506 MeV, $5/2_1^+ \to 1/2_1^+$	
	57	0.640(31)	−11.0(47)	+0.34(15)	0.877(14)	−1.73(345)	+0.05(11)
			Average $g(3/2_2^+)=+0.36(15)$			Average $g(5/2_1^+)=+0.048(92)$	
^{125}Te:			0.408 MeV, $3/2_2^+ \to 3/2_1^+$			0.428 MeV, $5/2_1^+ \to 3/2_1^+$	
	57	0.908(54)	−20.8(47)	+0.66(15)	1.829(34)	−7.33(169)	+0.235(54)
			0.444 MeV, $3/2_2^+ \to 1/2_1^+$			0.464 MeV, $5/2_1^+ \to 1/2_1^+$	
	57	0.461(41)	−0.055(6460)	+0.002(206)	0.967(32)	6.14(601)	−0.20(19)
			Average $g(3/2_2^+)=+0.43(12)$			Average $g(5/2_1^+)=+0.204(52)$	
						0.636 MeV, $5/2_2^+ \to 3/2_1^+$	
	57				0.108(89)	−20.1(617)	+0.70(210)
						0.672 MeV, $5/2_2^+ \to 1/2_1^+$	
	57				1.503(50)	6.61(788)	−0.23(27)
						Average $g(5/2_2^+)=-0.22(27)$	
^{110}Cd:			0.658 MeV, $2_1^+ \to 0_1^+$				
	66	3.009(16)	−15.0(9)	+0.379(23)			
	66	2.949(42)	−13.9(19)	+0.534(74)			
	66	2.825(25)	−9.49(74)	+0.365(29)			
			Average $g(2_1^+)=+0.382(17)$				

TABLE III. $g(^{110}\mathrm{Cd};2^+)$ obtained from radioactivity experiments.

Reference	g factor (in Ref.)	Mean life τ (ps) (in Ref.)	g factor recalculated with τ=7.73(7) ps[a]
21	0.30(12)	6.5(6)	0.252(101)
22	0.35(7)	6.6(6)	0.299(60)
23	0.28(5)	7.2(7)	0.261(47)
			Average: $g(2^+)=0.273(35)$

[a]Reference 24.

III. RESULTS

The energy level diagrams of the low-lying states of interest to this work, the measured $B(E2)$'s of selected ground state transitions, g factors measured by the transient field technique and g factors of isomeric states measured previously by other techniques, are shown in Figs. 8–10.

A. Odd-proton nuclei: ^{103}Rh and ^{107,109}Ag

The measurements, results, and analysis of the previously reported[4–6] Ag data are included here for completeness.

The $3/2_1^-$, 0.295 Mev and $5/2_1^-$, 0.357 MeV levels of ^{103}Rh were measured in the present investigation. The resulting g factors which depend on the choice of a pa-

TABLE IV. Summary of spectroscopic data and of g-factor measurements of selected states in ^{103}Rh, ^{107,109}Ag, ^{111,113}Cd, and ^{123,125}Te nuclei.

Isotope	E (MeV) J^π τ (ps)	$g(\frac{3}{2})$	E (MeV) J^π τ (ps)	$g(\frac{5}{2})$	$\frac{g(\frac{3}{2})}{g(\frac{5}{2})}$	Method[a]	Reference
^{103}Rh	0.295	+0.46(8)	+0.357	+0.37(8)	1.24(34)	TF	This work
	$3/2_1^-$	+0.54(5)	$5/2_1^-$	+0.43(3)	1.26(14)	TF	25,26
	9.7	+0.47(14)	85.1	0.38(13)	1.22(18)	RIG	27
^{107}Ag	0.325	+0.61(12)	0.423	+0.41(7)	1.49(31)	TF	4
	$3/2_1^-$	+0.63(9)	$5/2_1^-$	+0.37(6)	1.70(37)	TF	5
	7.2	+0.70(10)	51.4	+0.41(6)	1.70(35)	TF	6
		+0.51(7)		0.43(15)	1.12(29)	RIG	27[b]
^{109}Ag	0.311	+0.66(10)	0.415	+0.29(6)	2.30(48)	TF	4
	$3/2_1^-$	+0.77(10)	$5/2_1^-$	+0.36(5)	2.14(41)	TF	5
	8.5	+0.75(11)	47.6	+0.35(7)	2.14(53)	TF	6
		+0.56(18)		0.33(10)	1.66(33)	RIG	27[b]
^{111}Cd	0.342	+0.02(79)	0.620	+0.11(5)		TF	This work
	$3/2_1^+$		$5/2_2^+$				
	39.0		14.4				
^{113}Cd	0.298	−0.26(53)	0.584	+0.06(5)		TF	This work
	$3/2_1^+$		$5/2_2^+$				
	46.2		13.0				
^{123}Te	0.440	+0.36(15)	0.506	+0.05(9)		TF	This work
	$3/2_2^+$	+0.34(6)	$5/2_1^+$	+0.040(25)		IMPAC	28
	39.0		26.0				
^{125}Te	0.444	+0.43(12)	0.464	+0.20(5)		TF	This work
	$3/2_2^+$	+0.39(6)	$5/2_1^+$	+0.12(4)		IMPAC	28
	27.4		18.8				
			0.672	−0.22(27)		TF	This work
			$5/2_2^+$				
			1.9				

[a]Abbreviations TF and RIG stand for transient field and recoil in gas techniques, respectively. IMPAC refers to ion implantation perturbed angular correlation experiments.
[b]The results from Ref. 27 were normalized with respect to $g(^{110}\mathrm{Pd},2_1^+)=0.31(3)$ as described in Ref. 4.

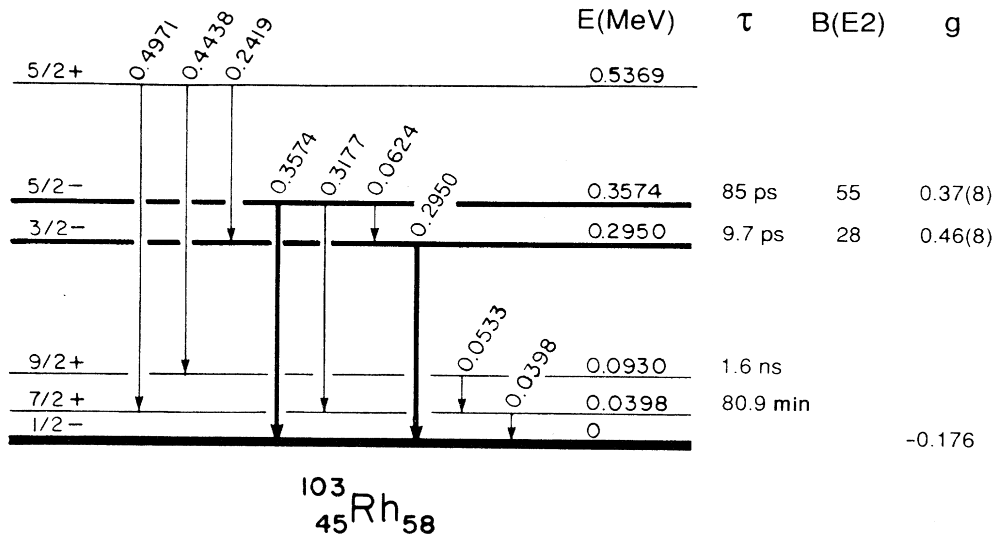

FIG. 8. Energy level diagram of the low-lying states of ^{103}Rh. The bold lines represent the gamma-ray transitions measured in this work. The values of the $B(E2)$'s in Weisskopf units assigned to a particular state correspond to the transition probability from that level to the ground state. The g factors listed for the short-lived state are those measured in this work. The g factors of the ground or isomeric states were taken from Ref. 31.

rametrization of the transient field, and the g factor ratios which are independent of a given parametrization, are displayed in Table IV together with the results obtained in other investigations.

B. Odd-neutron nuclei: ^{111,113}Cd and ^{123,125}Te

The g factors of the low-lying $\frac{3}{2}^+$ and $\frac{5}{2}^+$ states were determined from measurements of the precession of the gamma rays indicated by bold lines in Figs. 9 and 10. In addition, the spin of the 0.5056 MeV state in ^{123}Te has been unambiguously determined as $\frac{5}{2}$. Mixing ratios $\delta(E2/M1)$ for the $\frac{5}{2}\to\frac{3}{2}$, $\frac{3}{2}\to\frac{3}{2}$, and $\frac{3}{2}\to\frac{1}{2}$ transitions were extracted from the fits to the angular distributions and are listed in Table V.

The results for the Cd isotopes were obtained by normalizing the observed precessions to those measured for a

TABLE V. Summary of multipolarity mixing ratios.

Isotope	E_γ (MeV)	Transition	$\delta=(E2/M1)$	Reference
^{103}Rh	0.295	$3/2_1^- \to 1/2_1^-$	0.55(3)	This work
			$\lvert\delta\rvert=0.15$[a]	29
^{111}Cd	0.342	$3/2_1^+ \to 1/2_1^+$	−0.31(2),4.6(4)	This work
			$\lvert\delta\rvert=0.36$[a]	29
^{113}Cd	0.298	$3/2_1^+ \to 1/2_1^+$	−0.21(2), 3.0(1)[a]	This work
^{123}Te	0.159	$3/2_1^+ \to 1/2_1^+$	0.02–1.8	This work
			$\lvert\delta\rvert=0.084$[a]	29
	0.281	$3/2_2^+ \to 3/2_1^+$	−5.6– −0.1	This work
	0.347	$5/2_1^+ \to 3/2_1^+$	1.9	This work
	0.440	$3/2_2^+ \to 1/2_1^+$	0.1–1.7	This work
			$\lvert\delta\rvert=-2.1(1)$[a]	28
^{125}Te	0.408	$3/2_2^+ \to 3/2_1^+$	−1.9– −0.3	This work
			−1.6(1), 0.32(2)	28
	0.428	$5/2_1^+ \to 3/2_1^+$	1.1	This work
			−0.6(1)	28
			−0.95(2)	30
			$\lvert\delta\rvert=0.45$	29
	0.444	$3/2_2^+ \to 1/2_1^+$	0.04–1.9	This work
			−2.3(1)	28
	0.636	$5/2_2^+ \to 3/2_1^+$	−2.5– −0.9	This work

[a]These δ's were used to evaluate the $B(E2)$ transition probabilities quoted in Figs. 8–10.

similar target of ^{110}Cd measured under experimental conditions as close as possible to those pertaining to the odd Cd isotopes. The g factors of the ^{111,113}Cd isotopes normalized to that of ^{110}Cd(2^+) are displayed in Table IV.

No such calibrator exists in the Te isotopes. Hence the Rutgers parametrization was used to extract the final g factors for the Te isotopes. In principle, the g factor of the long-lived $3/2_1^+$, 0.159 MeV state in ^{123}Te, $g=0.48(8)$,[31] could be used to calibrate the transient field in the Te isotopes. The state is, however, only weakly excited by direct Coulomb excitation and the resulting angular precession cannot be measured with sufficient precision to extract a value for the transient field strength. The resulting g factors are shown in Table IV.

IV. DISCUSSION

A. Models

1. Single-particle model

Calculations of the magnetic moments of odd nuclei can be best carried out in the single-particle model, where the angular momentum characteristics of the odd particle in the appropriate shell level determine the g factor of the nucleus. Table VI lists these values for odd protons and odd neutrons in the $p_{1/2}$, $p_{3/2}$, $f_{5/2}$, $s_{1/2}$, $d_{3/2}$, and $d_{5/2}$ orbits which are relevant to the present nuclei. However, except for the g factor of the $5/2_1^+$ state in ^{103}Rh, the

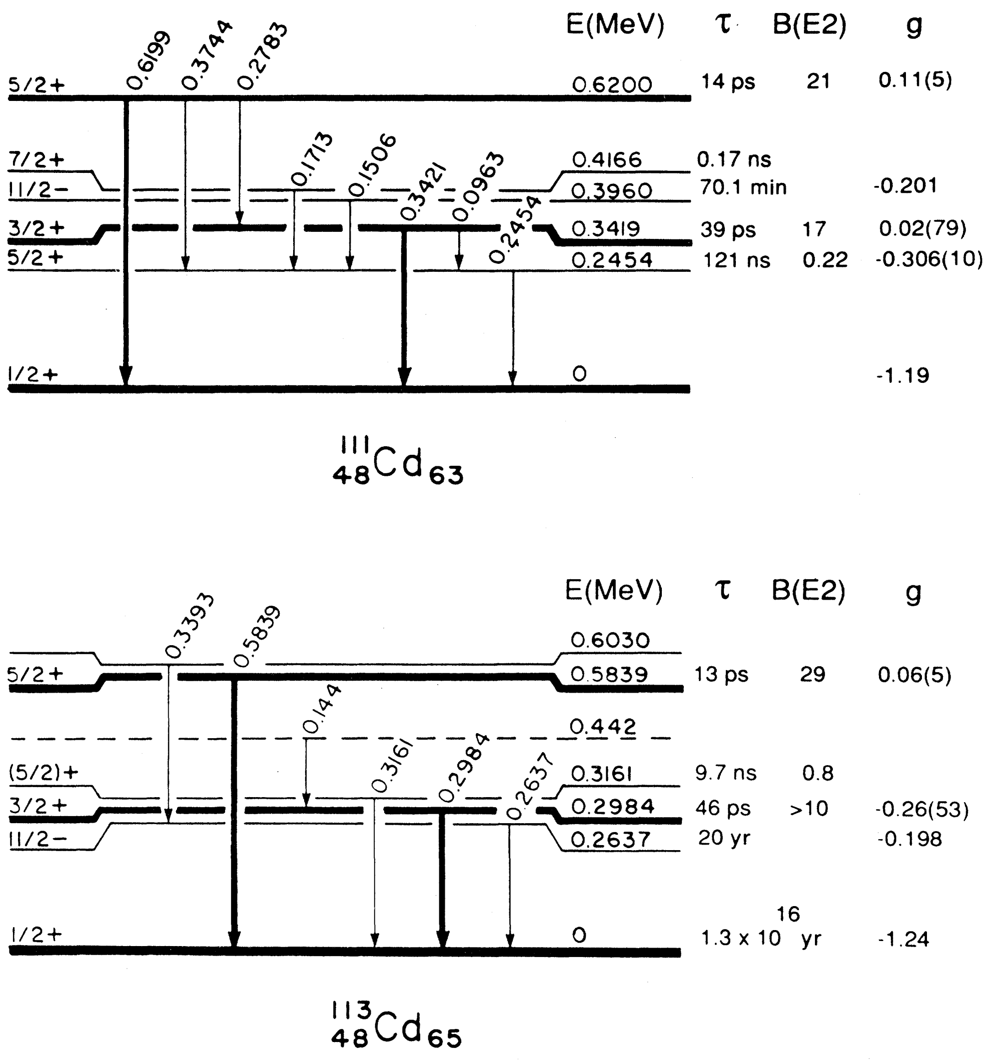

FIG. 9. Energy level diagram of the low-lying states of ^{111,113}Cd. The bold lines represent the gamma-ray transitions measured in this work. The values of the $B(E2)$'s in Weisskopf units assigned to a particular state correspond to the transition probability from that level to the ground state. The g factors listed for the short-lived state are those measured in this work. The g factors of the ground or isomeric states were taken from Ref. 31.

measured values are much smaller than the calculated single-particle values.

Magnetic moments are very sensitive to configuration admixtures. The single-particle energies of the neighboring even-even nuclei, ^{110,112}Cd and ^{122,124}Te, were calculated with the effective SKa Skyrme-type[32] interaction and a spherical constrained HF+BCS code.[33] The SKa force gives the right single-particle orbitals for Sn isotopes, and allows a reasonable to very good description of a wealth of nuclear properties in the mass region ($A \sim 100$). The result of these calculations shows that the energy difference of the single-particle states $(3s_{1/2})_\nu$ and $(2d_{3/2})_\nu$ ranges from $\Delta E \sim 0.5$ MeV for ^{112}Cd to $\Delta E \sim 0.15$ MeV for ^{124}Te. This result suggests that even at moderate values of the residual quadrupole interaction, the wave function of the valence particle in the $\frac{1}{2}^+$ ground state should contain admixtures of both orbitals. The ground state wave function can therefore be written as

$$|\tfrac{1}{2}^+\rangle_{\text{g.s.}} = \alpha|s_{1/2}\rangle + (1-\alpha^2)^{1/2}|(2^+ \otimes d_{3/2})\tfrac{1}{2}\rangle \ . \quad (8)$$

However, the mixing parameters that yield the observed ground state moments, $\alpha(^{111}\text{Cd}) = 0.53$ and $\alpha(^{125}\text{Te}) = 0.66$, are much too small to be realistic. The same approach, when applied to the $3/2_1^+$ state fails entirely, yielding $\alpha > 1$, independently of whether the $s_{1/2}$ configuration or the actual ground state wave function is mixed with the $d_{3/2}$ orbital. These results suggest more

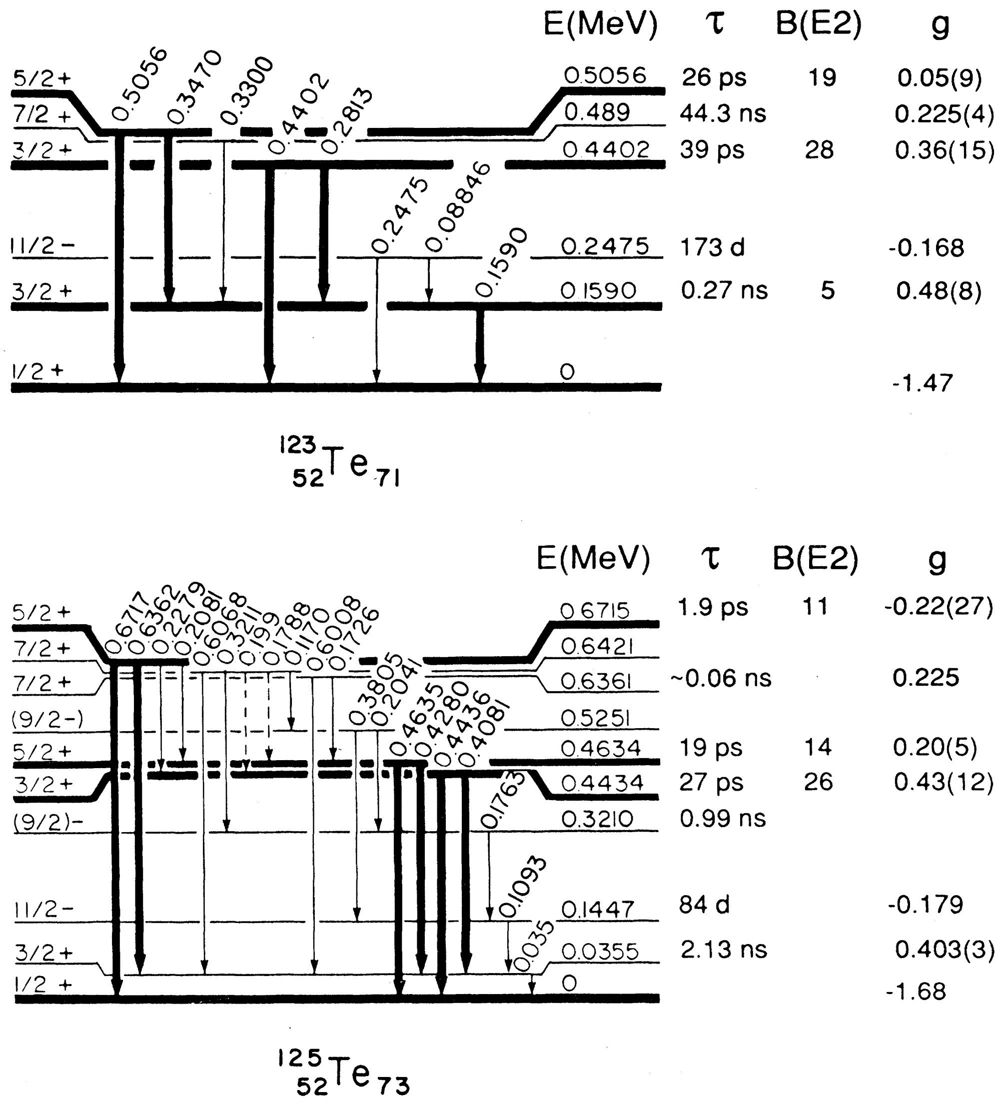

FIG. 10. Energy level diagram of the low-lying states of ^{123,125}Te. The bold lines represent the gamma-ray transitions measured in this work. The values of the $B(E2)$'s in Weisskopf units assigned to a particular state correspond to the transition probability from that level to the ground state. The g factors listed for the short-lived state are those measured in this work. The g factors of the ground or isomeric states were taken from Ref. 31.

TABLE VI. g factors in the independent single-particle model.

Configuration	Free nucleon g factors	Renormalized g factors	Renormalized g factors
	Proton		
	$g_l=1$	$g_l=1.1$	$g_l=1.1$
	$g_s=5.586$	$g_s=5$	$g_s=0.7$, $g_{\text{free}}=3.91$
$(p_{1/2})_\pi$	-0.529	-0.200	0.163
$(p_{3/2})_\pi$	$+2.529$	2.400	2.037
$(f_{5/2})_\pi$	$+0.345$	0.543	0.699
	Neutron		
	$g_l=0$		
	$g_s=-3.826$		
$(s_{1/2})_\nu$	-3.826		
$(d_{3/2})_\nu$	$+0.765$		
$(d_{5/2})_\nu$	-0.765		

complex configurations for the states of these odd nuclei.

A second approach was tried, which incorporates into the ground state a 1^+ excited state of the core as proposed by Arima and Horie:[34]

$$|jm\rangle\rangle=|jm\rangle+\epsilon|1^+j;jm\rangle\ , \tag{9}$$

$$|\tfrac{1}{2}^+\rangle_{\text{g.s.}}=\alpha|s_{1/2}\rangle\rangle+(1-\alpha^2)^{1/2}|(2^+\otimes d_{3/2})\tfrac{1}{2}\rangle\ . \tag{10}$$

The admixture parameter ϵ was taken from the measured magnetic moments in ^{115,119}Sn. The mixing parameters α obtained with these wave functions, $\alpha(^{113}\text{Cd})=0.803$ and $\alpha(^{125}\text{Te})=0.882$ are reasonable.

Another argument supports a single-particle assignment to the ^{123}Te, $3/2_1^+$ state. ^{123}I $(\frac{5}{2}^+)$ beta decays almost exclusively to the $3/2_1^+$ states of ^{123}Te by a Gamow-Teller $M1$ transition with a log $ft=5.5$, even though decay to other low-lying states is energetically favorable. As the ground state of ^{123}I is likely to be well described by a $(d_{3/2})_\pi$, the nature of the beta decay implies that the ^{123}Te $3/2_1^+$ state is also predominantly a $(d_{3/2})_\nu$ single-particle state. Similar arguments do not, however, apply to the Cd isotopes, where the lowest $\frac{3}{2}$ state might indeed be collective, as discussed in the next section.

Finally, magnetic moments can also be calculated within the framework of the quasiparticle model. A calculation carried out by Kisslinger and Sorensen[35] yielded $g(\frac{3}{2})=0.32$ and $g(\frac{5}{2})=0.04$.

2. *Weak-coupling model*

Collectivity can be achieved by coupling an odd particle (or hole) to the excited core of the neighboring even-even nucleus.[10] The g factor g_I of a state of spin I having such a configuration can readily be calculated from the coupling of the g factor of the odd particle (or hole), g_j, in its single-particle configuration and the g factor, g_c, of the excited core nucleus with spin I_c:

$$g_I=\frac{g_j}{2}\left[1+\frac{j(j+1)-I_c(I_c+1)}{I(I+1)}\right]+\frac{g_c}{2}\left[1-\frac{j(j+1)-I_c(I_c+1)}{I(I+1)}\right]\ . \tag{11}$$

In this approach it is realistic to take g_j as the measured moment of the ground state of the odd nucleus, and g_c as the measured moment of the core nucleus excited into the 2^+ state. The results of such calculations are shown in Table VII.

In the Te isotopes where the single-particle $(3s_{1/2})_\nu$ and $(2d_{3/2})_\nu$ states are nearly degenerate, the $\frac{3}{2}{}_1$ state maintains a predominantly single-particle structure while the higher $\frac{5}{2}{}_1$ and $\frac{3}{2}{}_2$ doublet can be assumed to correspond to the weak-coupling states. In the Cd isotopes these distinctions are less pronounced. The single-particle $(3s_{1/2})_\nu$ and $(2d_{3/2})_\nu$ states are 0.5 MeV apart. Thus the $\frac{3}{2}{}_1$ state appears higher in energy and may mix appreciably with the collective states.

3. *Axial and triaxial Nilsson models*

Both the axial and the triaxial Nilsson models have been invoked to explain the level scheme, and more recently the electromagnetic moments of the Ag isotopes.[4] The Nilsson model in its simplest form was not successful in predicting the observed moments. However, the introduction of triaxiality[11] yields results in fair agreement with observation. In particular, deformation and anisotropy parameters $\epsilon=0.26$ and $\gamma=20°-24°$ seem to give good agreement not only to the level scheme but also to the measured magnetic and quadrupole moments. Dejbakhsh *et al.*[40] carried out a very extensive analysis of energy levels and transition probabilities for ^{103}Rh, but have not calculated electromagnetic moments. Moment calculations have not been carried out either for the Cd or the Te isotopes.

4. *Interacting boson-fermion model (IBFM)*

The IBFM and supersymmetric extensions of the IBFM have been used to interpret level schemes of the Rh and Ag isotopes and magnetic moments of low-lying levels have been calculated.[26,14]

TABLE VII. Comparison of experimental g factors with g factors deduced in the weak-coupling scheme. The weak-coupling g factors were calculated by using the experimental ground state g factor of the odd nucleus and the following g factors for the core nuclei: $g(^{102}\mathrm{Ru},2^+)=0.371(31)$, Ref. 31, $g(^{104}\mathrm{Pd},2^+)=0.46(4)$, $g(^{110}\mathrm{Cd},2^+)=0.273(35)$, $g(^{112}\mathrm{Cd},2^+)=0.32(8)$, $g(^{114}\mathrm{Cd},2^+)=0.29(7)$, $g(^{122}\mathrm{Te},2^+)=0.33(3)$, $g(^{124}\mathrm{Te},2^+)=0.26(3)$, $g(^{126}\mathrm{Te},2^+)=0.19(3)$. The Pd and Cd data are from Ref. 36, and the Te data from Ref. 37. The Te isotopes were also measured by the transient field technique by Dunham and collaborators (Ref. 38) and by Hubler *et al.* by the IMPAC technique (Ref. 39), with very similar results to those quoted here. However, in the interest of consistency, only the Rutgers transient field data were used for the comparisons shown in the table.

Isotope	Expt. (*this work)	Calculation	
^{103}Rh		$^{102}\mathrm{Ru}\otimes p_{1/2}$	$^{104}\mathrm{Pd}\otimes p_{1/2}$
*$g(3/2_1^-)$	+0.46(8)	+0.480(37)	+0.587(48)
*$g(5/2_1^-)$	+0.37(8)	+0.262(25)	+0.333(32)
$\frac{g(3/2_1^-)}{g(5/2_1^-)}$	1.24	1.83	1.76
^{111}Cd		$^{110}\mathrm{Cd}\otimes s_{1/2}$	$^{112}\mathrm{Cd}\otimes s_{1/2}$
*$g(3/2_1^+)$	+0.02(79)	+0.566(42)	+0.622(96)
$g(5/2_1^+)$	−0.306(10)	−0.020(28)	+0.018(64)
*$g(5/2_2^+)$	+0.11(5)		
^{113}Cd		$^{112}\mathrm{Cd}\otimes s_{1/2}$	$^{114}\mathrm{Cd}\otimes s_{1/2}$
*$g(3/2_1^+)$	−0.26(53)	+0.633(96)	+0.597(84)
$g(5/2_1^+)$		+0.007(64)	−0.017(56)
*$g(5/2_2^+)$	+0.06(5)		
^{123}Te		$^{122}\mathrm{Te}\otimes s_{1/2}$	$^{124}\mathrm{Te}\otimes s_{1/2}$
$g(3/2_1^+)$	+0.48(8)	+0.69(36)	+0.607(36)
*$g(3/2_2^+)$	+0.36(15)		
*$g(5/2_1^+)$	+0.05(9)	−0.031(24)	−0.087(24)
^{125}Te		$^{124}\mathrm{Te}\otimes s_{1/2}$	$^{126}\mathrm{Te}\otimes s_{1/2}$
$g(3/2_1^+)$	+0.403(3)	+0.667(36)	+0.583(36)
*$g(3/2_2^+)$	+0.43(12)		
*$g(5/2_1^+)$	+0.20(5)	−0.147(24)	−0.203(24)
*$g(5/2_2^+)$	−0.22(27)		

B. Comparison with experimental data

1. Odd-proton nuclei

The comprehensive study of the Ag nuclei which described most structure characteristics such as energy levels, transition probabilities, and electromagnetic moments,[4] and which suggested that the addition of a proton to the vibrational neighboring even-even core produces a triaxial rotor with prolate deformation, was equally successful in understanding the ^{103}Rh spectra.[40] This latter analysis should be extended to include calculations of electromagnetic moments.

IBFM-1 calculations[26] of the ^{103}Rh energy levels and transition probabilities agree reasonably with experiment, but also suggest possible changes in the core such as those considered in the asymmetric rotor model, and support the possibility of γ softness in these nuclei.

The weak-coupling calculations predict moments in fair agreement with the observed ^{103}Rh g factors. However, unlike the case of the Ag isotopes, the ratio of $g(\frac{3}{2})/g(\frac{5}{2})$, which is fairly independent of systematic errors and experimental uncertainties, deviates considerably from the weak-coupling scheme.

2. Odd-neutron nuclei

The measurements of the magnetic moments of the short-lived low-lying states of ^{111,113}Cd and ^{123,125}Te nuclei complete the systematics in a region that has been thoroughly studied and where moments of long-lived isomers are well known. A clear signature of an evolution of nuclear structure as neutrons are added does not emerge from these data. The multiplicity of the $\frac{3}{2}$ and $\frac{5}{2}$ states suggests, however, that these nuclei have a fairly complex structure and may contain both single-particle configurations and collective degrees of freedom. Consider, for example, the states in ^{111}Cd that have large $B(E2)$ transition probabilities ($3/2_1^+$ and $5/2_2^+$). These states have magnetic moments that agree roughly with the picture of weak coupling of the odd neutron to the collective vibrational 2_1^+ core of the neighboring even nucleus (Table VII). On the other hand, the state for which $B(E2)$ is small, the $5/2_1^+$ state, has a negative magnetic moment that corresponds more closely to that of a single odd $d_{5/2}$ neutron (Table VI). Thus while some states can clearly be described by the behavior of a single independent nucleon, these states coexist with collective states described by weak coupling of the odd nucleon to the excited core of the neighboring nuclei or some other form of collective structure. In ^{113}Cd, while the g factor of the $5/2_2^+$ state agrees reasonably well with weak-coupling predictions, the moment of the $3/2_1^+$ state is much smaller than the weak-coupling schemes or the single-particle model predict. Similarly in the ^{123,125}Te isotopes, the moments of the $5/2_1^+$ and $5/2_2^+$ states, respectively do agree with weak coupling, but the moments of the $\frac{3}{2}^+$ states are smaller than any of the predictions. Additional experimental multipole branching ratios and theoretical work are required for a complete understanding of the structure of these nuclei.

V. CONCLUSIONS

Magnetic moments of odd-proton and odd-neutron medium-weight nuclei have been measured in order to understand the coupling of an odd nucleon to the even-even core. Specific structures can be associated with particular nuclei. The odd-proton Rh and Ag nuclei seem to acquire an asymmetric shape as a proton is added to the even Ru or Pd nucleus. In the Cd and Te isotopes, single-particle configurations appear to coexist with collective core excited states. More extensive calculations as well as more measurements are required to distinguish between various possible models for these nuclei.

ACKNOWLEDGMENTS

This work was supported in part by the National Science Foundation. We wish to thank A. Lipski for preparing the targets. One of us (L.Z.) acknowledges support from the U.S. Department of Energy, and one (D.B.) is grateful for a John von Neumann Supercomputing Postdoctural Fellowship.

*Permanent address: AT&T Bell Laboratories, Holmdel, NJ 07733-1988.

†Permanent address: Department of Physics, University of Ioannina, Ioannina, Greece.

‡Permanent address: Logica Space and Defence, London, England.

[1]E. Recknagel, in *Nuclear Spectroscopy and Reactions,* edited by J. Cerny (Academic, New York, 1974), Part C.

[2]N. Benczer-Koller, M. Hass, and J. Sak, Annu. Rev. Nucl. Part. Sci. **30**, 53 (1980); N. K. B. Shu, D. Melnick, J. M. Brennan, W. Semmler, and N. Benczer-Koller, Phys. Rev. C **21**, 1828 (1980).

[3]A. Wolf, D. D. Warner, and N. Benczer-Koller, Phys. Lett. **158B**, 7 (1985).

[4]D. Ballon, Y. Niv, S. Vajda, N. Benczer-Koller, L. Zamick, and G. Leander, Phys. Rev. C **33**, 1461 (1986).

[5]A. E. Stuchbery, L. D. Wood, R. A. Bark, and H. H. Bolotin, Hyp. Int. **20**, 119 (1984).

[6]D. Bazzacco, F. Brandolini, P. Pavan, C. Rossi-Alvarez, R. Zannoni, and M. de Poli, Nuovo Cimento **84**, 106 (1984).

[7]O. Häusser, H. R. Andrews, D. Ward, N. Rud, P. Taras, R. Nicole, J. Keinonen, P. Skensved, and C. V. Stager, Nucl. Phys. **A406**, 339 (1983).

[8]A. E. Stuchbery, L. D. Wood, H. H. Bolotin, C. E. Doran, I. Morrison, A. B. Byrne, and G. J. Lampard, Nucl. Phys. **A486**, 374 (1988).

[9]D. Bazzacco, F. Brandolini, K. Loewenich, P. Pavan, C. Rossi-Alvarez, R. Zannoni, and M. de Poli, Phys. Rev. C **33**, 1785 (1986).

[10]A. deShalit, Phys. Rev. **122**, 1500 (1961).

[11]Ch. Vieu, S. E. Larsson, G. Leander, I. Ragnarsson, and J. S. Dionisio, Phys. Rev. C **22**, 853 (1980).

[12]F. Iachello and O. Scholten, Phys. Rev. Lett. **43**, 679 (1979).

[13]J. Jolie, P. Van Isacker, K. Heyde, J. Moreau, G. Van Landeghem, M. Waroquier, and O. Scholten, Nucl. Phys. **A438**, 15 (1985).

[14]L. D. Wood, H. H. Bolotin, I. Morrison, R. A. Bark, H. Yamada, and A. E. Stuchbery, Nucl. Phys. **A427**, 639 (1984).

[15]G. Lenner, R. Tanczyn, A. Pakou, D. Barker, A. Piqué, G. Kumbartzki, and N. Benczer-Koller, Bull. Am. Phys. Soc. **32**, 1562 (1987).

[16]R. Tanczyn, G. Lenner, A. Pakou, A. Piqué, G. Kumbartzki, D. Berdichevsky, L. Zamick, and N. Benczer-Koller, Bull. Am. Phys. Soc. **33**, 1584 (1988).

[17]N. Benczer-Koller, *Shell Model and Nuclear Structure: where do we stand?* (World Scientific, Singapore, 1989).

[18]N. Benczer-Koller, G. Lenner, R. Tanczyn, A. Pakou, G. Kumbartzki, and A. Piqué, Hyp. Int. **43**, 457 (1988).

[19]A. Piqué, J. M. Brennan, R. Darling, R. Tanczyn, D. Ballon, and N. Benczer-Koller, Nucl. Instrum. Methods (to be published).

[20]H. L. Rose and D. M. Brink, Rev. Mod. Phys. **39**, 306 (1967).

[21]L. Keszthelyi, I. Demeter, I. Dézsi, and L. Varga, in *Hyperfine Structure and Nuclear Radiations,* edited by E. Matthiass and D. Shirley (North-Holland, Amsterdam, 1968), p. 155.

[22]K. Johansson, E. Karlsson, L.O. Norlin, R. A. Windahl, and M. R. Ahmed, Nucl. Phys. **A188**, 600 (1972).

[23]G. W. Wang, A. J. Becker, L. M. Chirovsky, J. L. Groves, and C. S. Wu, Phys. Rev. C **18**, 476 (1978).

[24]P. de Gelder, E. Jacobs, and D. DeFrenne, Nucl. Data Sheets **38**, 545 (1983).

[25]G. J. Lampard, H. H. Bolotin, C. E. Doran, and A. E. Stuchbery, Australian National University, Research School of Physical Sciences, Canberra, Annual Report, 1987.

[26]G. J. Lampard, H. H. Bolotin, C. E. Doran, L. D. Wood, I. Morrison, and A. E. Stuchbery, Nucl. Phys. (to be published).

[27]T. R. Miller, P. D. Bond, W. A. Little, S. M. Lazarus, M. Takeda, G. D. Sprouse, and S. S. Hanna, Suppl. J. Phys. Soc. Jpn. **34**, 107 (1973).

[28]W. M. Roney, D. W. Gebbie, and R. R. Borchers, Nucl. Phys. **A236**, 165 (1974).

[29]*Table of Isotopes,* edited by C. M. Lederer and V. S. Shirley (Wiley, New York, 1978).

[30]M. Rots, R. Silverans, and R. Coussement, Nucl. Phys. **A170**, 240 (1971).

[31]P. Raghavan, At. Data Nucl. Data Tables (to be published).

[32]H. S. Köhler, Nucl. Phys. **A258**, 301 (1976).

[33]D. Berdichevsky, R. Fleming, D. W. L. Sprung, F. Tondeur, Z. Phys. A **329**, 393 (1988); D. Berdichevsky and W. Reisdorf, *ibid.* **327**, 217 (1987).

[34]A. Arima and H. Horie, Prog. Theor. Phys. **11**, 509 (1954); **12**, 623 (1954).

[35]L. Kisslinger and R. Sorensen, Rev. Mod. Phys. **35**, 853 (1963).

[36]J. M. Brennan, M. Hass, N. K. B. Shu, and N. Benczer-Koller, Phys. Rev. C **21**, 574 (1980).

[37]N. K. B. Shu, R. Levy, N. Tsoupas, A. Lopez-Garcia, W. Andrejtscheff, and N. Benczer-Koller, Phys. Rev. C **24**, 954 (1981).

[38]J. S. Dunham, R. T. Westervelt, R. Avida, and S. S. Hanna (private communication); J. L. Thornton, B. T. Neyer, and S. S. Hanna, Bull. Am. Phys. Soc. **30**, 1264 (1985).

[39]G. K. Hubler, H. W. Kugel, and D. E. Murnick, Phys. Rev. C **9**, 1954 (1974).

[40]H. Dejbakhsh, R. P. Schmitt, and G. Mouchaty, Phys. Rev. C **37**, 621 (1988).